A mixed Fourier–Galerkin–finite-volume method to solve the fluid dynamics equations in cylindrical geometries

Article *in* Fluid Dynamics Research · June 2012

DOI: 10.1088/0169-5983/44/3/031414

CITATIONS
4

READS
141

3 authors:

Jose Nunez
Universidad Nacional Autónoma de México
23 PUBLICATIONS **28** CITATIONS
SEE PROFILE

Eduardo Ramos
Instituto Tecnológico Superior de Ciudad Constitución (ITSCC)
89 PUBLICATIONS **265** CITATIONS
SEE PROFILE

Juan Lopez
Arizona State University
229 PUBLICATIONS **4,005** CITATIONS
SEE PROFILE

IOP PUBLISHING FLUID DYNAMICS RESEARCH

Fluid Dyn. Res. **44** (2012) 031414 (10pp) doi:10.1088/0169-5983/44/3/031414

A mixed Fourier–Galerkin–finite-volume method to solve the fluid dynamics equations in cylindrical geometries

Jóse Núñez[1], **Eduardo Ramos**[1] **and Juan M Lopez**[2]

[1] Centro de Investigación en Energía, Universidad Nacional Autónoma de México, Ap.P. 34, 62580 Temixco Morelos, Mexico
[2] School of Mathematical and Statistical Sciences, Arizona State University, Tempe, AZ 85287, USA

E-mail: jnegl@cie.unam.mx

Received 21 October 2011, in final form 9 February 2012
Published 23 May 2012
Online at stacks.iop.org/FDR/44/031414

Communicated by E Knobloch

Abstract

We describe a hybrid method based on the combined use of the Fourier Galerkin and finite-volume techniques to solve the fluid dynamics equations in cylindrical geometries. A Fourier expansion is used in the angular direction, partially translating the problem to the Fourier space and then solving the resulting equations using a finite-volume technique. We also describe an algorithm required to solve the coupled mass and momentum conservation equations similar to a pressure-correction SIMPLE method that is adapted for the present formulation. Using the Fourier–Galerkin method for the azimuthal direction has two advantages. Firstly, it has a high-order approximation of the partial derivatives in the angular direction, and secondly, it naturally satisfies the azimuthal periodic boundary conditions. Also, using the finite-volume method in the r and z directions allows one to handle boundary conditions with discontinuities in those directions. It is important to remark that with this method, the resulting linear system of equations are band-diagonal, leading to fast and efficient solvers. The benefits of the mixed method are illustrated with example problems.

(Some figures may appear in colour only in the online journal)

1. Introduction

Several numerical algorithms for solving the fluid dynamics equations in cylindrical coordinates are currently available in the literature. The well-known discretization methods, finite difference and finite volume, have been used and explained in several reports (Eggels

0169-5983/12/031414+10$33.00

et al 1994, Verzicco and Orlandi 1996, Fukagata and Kasagi 2002). The convenience of using discretization schemes such as central differences, high-order compact or energy-conservative has been frequently explored in this context and also different treatments to avoid the singularity at the origin of coordinates have been presented and discussed. The decoupling strategies examined include the fractional step or projection method (Chorin 1968) and the SIMPLE algorithm (Patankar and Spalding 1972). With these methods, it is possible to find the solution to the pressure equation by a sequence of steps.

If the system under analysis can be conveniently described in terms of a spatially cyclic coordinate, the harmonic functions used in spectral methods are the natural basis to represent the dependent variables since those functions automatically and individually satisfy the periodic conditions. The Fourier representation and the corresponding identification of the expansion coefficients are the basic idea underlying the spectral methods. An advantage of this representation is that for an equivalent computational effort, the solution is more accurate since the error decays exponentially. For this reason, Fourier spectral methods have been used for direct numerical simulations of turbulent flows (Canuto *et al* 1988) or as a tool for stability analysis in fluid flows (Lopez *et al* 2007). In most works, the spatial discretization for the azimuthal direction is done with Fourier series, while Chebyshev or Legendre polynomials are used for the radial and axial directions (Gottlieb and Orzag 1977, Peyret 2002). The pressure–velocity decoupling strategies that have been used with the spectral methods representation are, for example, projection methods (Brown *et al* 2001) and influence matrix (Tuckerman 1989). In spite of their advantages, spectral methods are not well suited for problems with discontinuities in the axial or radial directions owing to the occurrence of the Gibbs phenomenon. Another relevant feature that must be considered is that the linear system of equations resulting from spectral methods is full and, consequently, more difficult to solve than the band linear system of equations obtained with the finite-volume discretization.

A combined formulation that includes finite-volume and Fourier spectral methods can take advantage of the two techniques. Barbosa and Daube (2005) implemented a mixed Fourier/finite-difference method to solve fluid dynamics equations in cylindrical geometries. Their work is closely related to the present study and deserves a somewhat more detailed description. The integration is based on the use of mimetic discrete first-order operators (divergence, gradient, curl). The nonlinear terms were discretized in such a way that they are energetically neutral. No artificial boundary conditions are required on the axis $r = 0$ since they used an *ad hoc* definition for the divergence operator at the centers of the cells adjacent to the axis, and for the definition of the axial component of the vorticity on the axis. The velocity–pressure coupling is handled by means of an incremental projection method. It must be observed, however, that these fractional step methods introduce an error in the tangential component of the velocity along the boundary, which is sometimes referred to as a spurious numerical boundary layer.

In this paper, we propose a mixed method to solve the conservation equations in a cylindrical domain. Fourier expansion is used in the azimuthal direction and finite-volume discretization in the radial and axial directions. Also, we implement a pressure correction method to handle velocity–pressure coupling in the fluid dynamics equations. The idea is to calculate pressure and velocity corrections for each Fourier mode of the expansion until mass conservation is satisfied. This can be done since the linear system of equations of the finite-volume discretization is sparse and band diagonal due to the local approximation. Although this decoupling strategy has been used in applications for heat transfer problems for finite difference methods, apparently it has not been applied before for spectral methods.

2. Conservation equations and Fourier expansion

The conservation equations for an incompressible fluid in cylindrical coordinates (θ, r, z) with velocity (u, v, w) can be written as

$$\frac{\partial v}{\partial t} + (\vec{u}\cdot\nabla)v - \frac{u^2}{r} = -\frac{\partial p}{\partial r} + \Gamma\left(\nabla^2 v - \frac{v}{r^2} - \frac{2}{r^2}\frac{\partial u}{\partial \theta}\right) + f_r, \tag{1}$$

$$\frac{\partial u}{\partial t} + (\vec{u}\cdot\nabla)u + \frac{uv}{r} = -\frac{1}{r}\frac{\partial p}{\partial \theta} + \Gamma\left(\nabla^2 u - \frac{u}{r^2} + \frac{2}{r^2}\frac{\partial v}{\partial \theta}\right) + f_\theta, \tag{2}$$

$$\frac{\partial w}{\partial t} + (\vec{u}\cdot\nabla)w = -\frac{\partial p}{\partial z} + \Gamma\nabla^2 w + f_z, \tag{3}$$

$$\frac{1}{r}\frac{\partial}{\partial r}(rv) + \frac{1}{r}\frac{\partial u}{\partial \theta} + \frac{\partial w}{\partial z} = 0, \tag{4}$$

where

$$\vec{u}\cdot\nabla = v\frac{\partial}{\partial r} + \frac{u}{r}\frac{\partial}{\partial \theta} + w\frac{\partial}{\partial z} \tag{5}$$

and

$$\nabla^2 = \frac{1}{r}\frac{\partial}{\partial r}\left(r\frac{\partial}{\partial r}\right) + \frac{1}{r^2}\frac{\partial^2}{\partial \theta^2} + \frac{\partial^2}{\partial z^2}. \tag{6}$$

The governing equations are written in dimensionless form, using Γ as a generalized dimensionless parameter.

We start by rewriting the equations for the velocity components in a convenient form for the analysis. The expression for the azimuthal velocity component is

$$\frac{\partial u}{\partial t} + N_u = -\frac{1}{r}\frac{\partial p}{\partial \theta} + \Gamma\left(\nabla^2 u - \frac{u}{r^2}\right) + f_u, \tag{7}$$

where

$$N_u = (\vec{u}\cdot\nabla)u + \frac{uv}{r} \tag{8}$$

is the nonlinear term and

$$f_u = \frac{2\Gamma}{r^2}\frac{\partial v}{\partial \theta} + f_\theta \tag{9}$$

is the body force plus terms that arise in the cylindrical coordinate formulation. Similar expressions can be written for the axial and radial components.

We approximate the velocity, pressure, N and f with truncated Fourier series expansions in the azimuthal direction as follows:

$$u = \sum_{k=-K/2}^{K/2-1} \hat{u}_k(r,z)\,\mathrm{e}^{\mathrm{i}k\theta}, \quad v = \sum_{k=-K/2}^{K/2-1} \hat{v}_k(r,z)\,\mathrm{e}^{\mathrm{i}k\theta}, \quad w = \sum_{k=-K/2}^{K/2-1} \hat{w}_k(r,z)\,\mathrm{e}^{\mathrm{i}k\theta}, \quad \theta\in[0,2\pi), \tag{10}$$

$$p = \sum_{k=-K/2}^{K/2-1} \hat{p}_k(r,z)\,\mathrm{e}^{\mathrm{i}k\theta}, \quad N = \sum_{k=-K/2}^{K/2-1} \hat{N}_k(r,z)\,\mathrm{e}^{\mathrm{i}k\theta}, \quad f = \sum_{k=-K/2}^{K/2-1} \hat{f}_k(r,z)\,\mathrm{e}^{\mathrm{i}k\theta}, \quad \theta\in[0,2\pi), \tag{11}$$

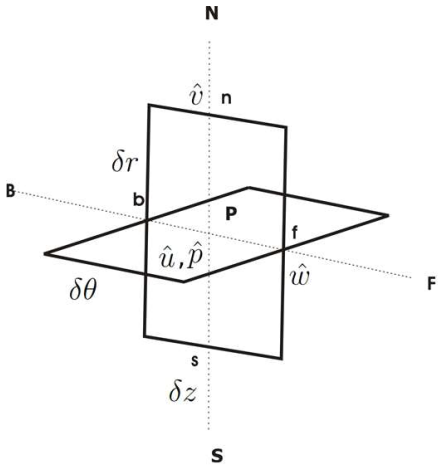

Figure 1. Staggered arrangement for the Fourier mode coefficients.

where $\hat{u}_k$, $\hat{v}_k$, $\hat{w}_k$, $\hat{N}_k$ and $\hat{f}_k$ are the Fourier expansion coefficients of the corresponding variables. Since all functions are real, the Fourier expansion coefficients have the following properties: $\hat{u}_{-K/2}$ is real and $\hat{u}_k = \bar{\hat{u}}_k$ for $k = 0, 1, \ldots, K/2 - 1$. A 3/2 rule aliasing removing technique has been used.

3. Discrete equations

Substituting Fourier expansions for the velocity given in equation (10) into the mass conservation (equation (4)), the following expression is obtained:

$$\frac{\mathrm{i}k}{r}\hat{u} + \frac{1}{r}\frac{\partial}{\partial r}(r\hat{v}) + \frac{\partial \hat{w}}{\partial z} = 0, \quad \text{for all } k. \tag{12}$$

For simplicity, the subindex k has been omitted and also the range for k is only specified when required to avoid confusion.

The resulting equations are discretized with the finite-volume method. All equations are integrated on a control volume (figure 1), where the integral over the volume is approximated by the middle-point rule. As is commonly implemented in finite-volume techniques, we use a staggered arrangement for the velocity components and scalar fields; in the present method we have used a staggered arrangement for the Fourier modes (see figure 1).

Using the notation of figure 1, the integration of the mass conservation equation is

$$\int_V \left(\frac{\mathrm{i}k}{r}\hat{u} + \frac{1}{r}\frac{\partial}{\partial r}(r\hat{v}) + \frac{\partial \hat{w}}{\partial z}\right) \mathrm{d}V = \frac{\mathrm{i}k}{r_P}\hat{u}_P \delta V + \frac{1}{r_P}\frac{r_n\hat{v}_n - r_s\hat{v}_s}{\delta r}\delta V + \frac{\hat{w}_f - \hat{w}_b}{\delta z}\delta V,$$

$$= \frac{\mathrm{i}k}{r_P}\hat{u}_P \delta V + \hat{v}_n A_n - \hat{v}_s A_s + \hat{w}_f A_s - \hat{w}_b A_b = 0 \tag{13}$$

where $\delta V = r_P \delta r \delta\theta \delta z$, $A_n = r_n \delta\theta \delta z$, $A_s = r_s \delta\theta \delta z$, $A_P = r_P \delta\theta \delta z$, and $A_f = A_b = r_P \delta r \delta\theta$.

The equation for the u-component is written in terms of the Fourier modes, with the time derivative approximated using the semi-implicit Euler method, where the linear terms on the main variable in the equation are treated implicitly and the rest of the linear terms and all the

nonlinear terms are treated explicitly:

$$\frac{\hat{u}-\hat{u}^0}{\delta t}+\hat{N}_u^0=-\frac{\mathrm{i}k}{r}\hat{p}+\Gamma\left(\frac{1}{r}\frac{\partial}{\partial r}\left(r\frac{\partial\hat{u}}{\partial r}\right)-\frac{k^2+1}{r^2}\hat{u}+\frac{\partial^2\hat{u}}{\partial z^2}\right)+\hat{f}_u^0. \tag{14}$$

Rearranging, we have

$$\left(\frac{1}{\delta t}+\Gamma\frac{k^2+1}{r^2}\right)\hat{u}=-\frac{\mathrm{i}k}{r}\hat{p}+\Gamma\left(\frac{1}{r}\frac{\partial}{\partial r}\left(r\frac{\partial\hat{u}}{\partial r}\right)+\frac{\partial^2\hat{u}}{\partial z^2}\right)+\hat{f}_u^0-\hat{N}_u^0+\frac{\hat{u}^0}{\delta t}. \tag{15}$$

Observe that the time integration scheme used implies that a Stokes-like problem is solved at each time step.

Integrating over a control volume gives

$$\left(\frac{1}{\delta t}+\Gamma\frac{k^2+1}{r_P^2}\right)\hat{u}_P\delta V=\Gamma\left(\frac{\hat{u}_N-\hat{u}_P}{\delta r}A_n-\frac{\hat{u}_P-\hat{u}_S}{\delta r}A_s+\frac{\hat{u}_F-\hat{u}_P}{\delta z}A_f-\frac{\hat{u}_P-\hat{u}_B}{\delta z}A_b\right)$$
$$+\left(\hat{f}_{u_P}^0-\hat{N}_{u_P}^0+\frac{\hat{u}_P^0}{\delta t}\right)\delta V-\frac{\mathrm{i}k}{r_P}\hat{p}_P\delta V, \tag{16}$$

which can be expressed as the following linear system:

$$a_P^u\hat{u}_P=a_N^u\hat{u}_N+a_S^u\hat{u}_S+a_F^u\hat{u}_F+a_B^u\hat{u}_B+S_P^u-\frac{\mathrm{i}k}{r_P}\hat{p}_P\delta V, \tag{17}$$

where

$$a_N^u=\Gamma\frac{A_n}{\delta r},\quad a_S^u=\Gamma\frac{A_s}{\delta r},\quad a_F^u=\Gamma\frac{A_f}{\delta z},\quad a_B^u=\Gamma\frac{A_b}{\delta z}, \tag{18}$$

$$a_P^u=a_N^u+a_S^u+a_F^u+a_B^u+\left(\frac{1}{\delta t}+\Gamma\frac{k^2+1}{r_P^2}\right)\delta V, \tag{19}$$

$$S_P^u=\left(\hat{f}_{u_P}^0-\hat{N}_{u_P}^0+\frac{\hat{u}_P^0}{\delta t}\right)\delta V. \tag{20}$$

The nonlinear terms in the conservation of momentum equations are part of the source terms in the discretized equations. The nonlinear terms are calculated with a central difference scheme. Other approximations, such as upwind or QUICK, could be used since the central scheme might lead to unphysical oscillations if the discretization is too coarse.

The nonlinear terms must be expressed in Fourier modes, and the most convenient way to do this is to calculate the products in physical space and then Fourier transform the products.

Applying analogous approximations and discretizations to the radial momentum conservation equation (v—velocity component) and axial momentum conservation equation (w—velocity component), the full set of discretized equations is formed:

$$a_P^u\hat{u}_P=\sum_{nb}a_{nb}^u\hat{u}_{nb}+S_P^u-\frac{\mathrm{i}k}{r_P}\hat{p}_P\delta V, \tag{21}$$

$$a_P^v\hat{v}_P=\sum_{nb}a_{nb}^v\hat{v}_{nb}+S_P^v-(\hat{p}_N-\hat{p}_P)A_p \tag{22}$$

and

$$a_P^w\hat{w}_P=\sum_{nb}a_{nb}^w\hat{w}_{nb}+S_P^w-(\hat{p}_F-\hat{p}_P)A_f. \tag{23}$$

The expressions for the coefficients of the linear system of equations for v and w equations ($a_P^v, a_P^w, \ldots$) are similar to equations (18)–(20).

Given that momentum equations for each of the Fourier modes decouple, this algorithm is a natural candidate for parallelization.

3.1. Axis treatment

Different treatments for the radial velocity at the origin have been proposed by many authors in the context of the finite-volume discretization method (Eggels *et al* 1994, Fukagata and Kasagi 2002). These strategies can also be implemented in the present formulation for the Fourier mode equations. Frequently, an artificial boundary condition for the radial velocity v at the origin is used. Two examples are the Neumann-like condition $v(i, 0, k) = v(i, 1, k)$ and the streamwise average of the radial velocities $v(i, 0, k) = ((v(i, 1, k) - v(i + n_\theta/2, 1, k))/2$.

4. Pressure–velocity decoupling strategy

There are many decoupling strategies for the fluid dynamics equations. One of these methods is known as the SIMPLE method (Patankar and Spalding 1972).

Let $\hat{p}^*$ denote an initial guess for pressure, according to expressions (21), (22) and (23); the velocity corresponding to the solution with such a pressure field is called $\hat{u}^*$, $\hat{v}^*$ and $\hat{w}^*$. These solutions do not satisfy the incompressibility condition. The pressure and velocity corrections ($\hat{p}'_k, \hat{u}'_k$) are defined by

$$\hat{p}_k = \hat{p}_k^* + \hat{p}'_k \tag{24}$$

and

$$\hat{u}_k = \hat{u}_k^* + \hat{u}'_k, \quad \hat{v}_k = \hat{v}_k^* + \hat{v}'_k, \quad \hat{w}_k = \hat{w}_k^* + \hat{w}'_k. \tag{25}$$

Applying the standard SIMPLE algorithm (Patankar and Spalding 1972) to each mode separately the following equation for the pressure correction is obtained:

$$a_P^p \hat{p}'_P = a_N^p \hat{p}'_N + a_S^p \hat{p}'_S + a_F^p \hat{p}'_F + a_B^p \hat{p}'_B + S_P, \tag{26}$$

where

$$a_N^p = (d_v)_n A_n, \quad a_S^p = (d_v)_s A_s, \tag{27}$$

$$a_F^p = (d_w)_f A_f, \quad a_B^p = (d_w)_b A_b, \tag{28}$$

$$a_P^p = a_N^p + a_S^p + a_F^p + a_B^p + \frac{k^2}{r_P^2} * d_u * \delta V, \tag{29}$$

$$S_P = -\left(\frac{\mathrm{i}k}{r_P}\hat{u}_P^* \delta V + \hat{v}_n^* A_n - \hat{v}_s^* A_s + \hat{w}_f^* A_s - \hat{w}_b^* A_b\right) \tag{30}$$

and

$$\mathrm{d}u = \frac{\delta V}{a_P^u - \sum_{nb} a_{nb}^u}, \quad \mathrm{d}v = \frac{A_p}{a_P^v - \sum_{nb} a_{nb}^v} \quad \text{and} \quad \mathrm{d}w = \frac{A_f}{a_P^w - \sum_{nb} a_{nb}^w}. \tag{31}$$

Note that the linear system of equations for the pressure correction contains complex numbers, but the entries of the matrix are real and therefore no calculations in the complex domain are necessary to solve the linear system.

Equations for the correction of the velocity components in terms of the pressure correction are obtained as

$$\hat{u}'_P = -d_u \frac{\mathrm{i}k}{r_P} \hat{p}'_P, \quad \hat{v}'_P = -d_v(\hat{p}'_N - \hat{p}'_P) \quad \text{and} \quad \hat{w}'_P = -d_w(\hat{p}'_F - \hat{p}'_P). \tag{32}$$

When the pressure correction equation is solved, the pressure and velocity are modified to get a better approximation. In the next iteration step, the updated values are used as initial guesses and the procedure is repeated until the velocity satisfies the divergence-free criterion.

The present method is based on the SIMPLE pressure decoupling strategy and therefore it is expected that it inherits its converging features, although a formal analysis would be required to demonstrate this statement.

5. Benchmark solutions

Two examples are presented to illustrate the applicability of the proposed methodology for the numerical solution of the Navier–Stokes equations in cylindrical domains. In these examples, one or more important characteristics that a robust method must have and a comparison of it with the corresponding numerical solution using a finite-volume method and a Fourier–Chebyshev spectral method are presented. The algorithms used for solving the example problems with a finite-volume method and a Fourier–Galerkin and Chebyshev spectral method can be found in the literature (Versteeg and Malalasekera 1995, Fukagata and Kasagi 2002, Peyret 2002, Mercader *et al* 2010).

5.1. Lid-driven flow

The first example is the lid-driven flow in a circular domain with the tangential velocity condition at the outer radius defined by $u = \cos\theta$ for a Reynolds number $Re = 400$; the conditions are the same as in Barbosa and Daube (2005). The motion of the boundary generates a flow with nonzero flow at $r = 0$ and therefore a correct calculation of the radial velocity at the origin is very important for an accurate numerical solution. In this particular calculation, the streamwise average condition (see section 3.1) strategy was used to avoid the singularity at the origin. The solution obtained with a Fourier–Chebyshev spectral method does not require any special treatment at the origin and can be used as a reference for a quantitative assessment. In order to illustrate the results, figure 2(a) shows a color map for the velocity magnitude and the corresponding streamlines. In figure 2(b), the radial velocity profiles on the line $\theta = \pi/4$ obtained from the two solution techniques are shown; the flow field around the origin is smooth and the two radial velocity profiles are in agreement. A more quantitative assessment of the difference between the two solutions is given in figure 2(c), where the normalized difference between the two solutions of figure 2(b) is shown. As can be seen, at the origin the two solutions differ by less than 5×10^{-3}.

We use the total kinetic energy $\mathcal{K}$ to compare the solutions obtained by the three different methods described previously. $\mathcal{K}$ is defined by

$$\mathcal{K} = \frac{1}{V} \int (u^2 + v^2)\, \mathrm{d}V, \tag{33}$$

where V is the volume occupied by the fluid. In principle, to determine the convergence of the approximate solution, it would be necessary to know *a priori* the exact solution, but such information is usually unknown. An alternative criterion for the grid convergence error of steady-state flows can be estimated from $\epsilon = |\mathcal{K}_n - \mathcal{K}_{n-1}|/\mathcal{K}_{n_{\max}}$, where n denotes the number

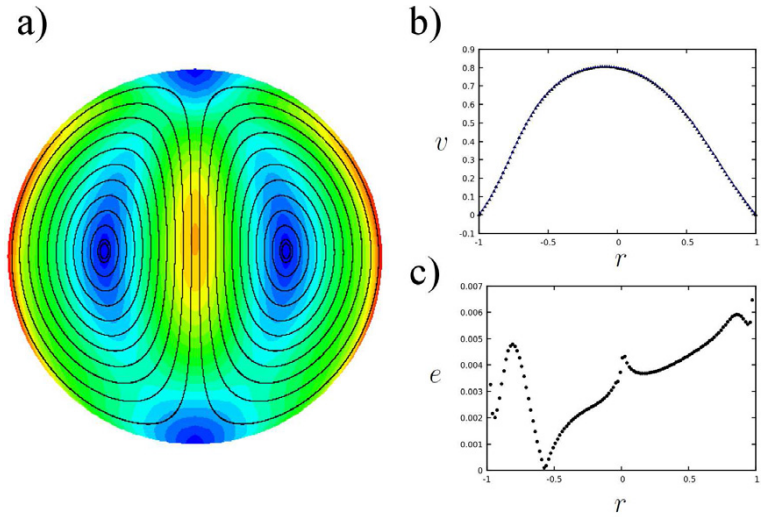

Figure 2. (a) Streamlines and magnitude of the velocity field for the lid-driven flow; (b) radial velocity profile at $\theta = \pi/4$, computed using the spectral method (continuous line) and the Fourier finite-volume method (triangular dots); and (c) the normalized difference between the results.

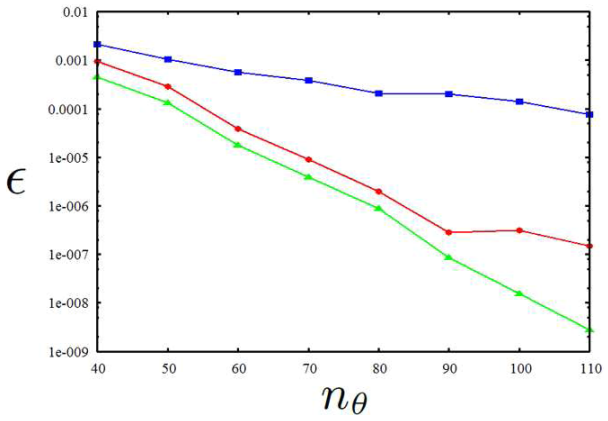

Figure 3. Relative convergence for a lid-driven flow as a function of n_θ, using the spectral method (green line), the Fourier/finite-volume method (red line) and the finite-volume method (blue line). In all cases, $n_r = 60$.

of points used in the discretization. This relative convergence criterion is shown in figure 3 for the three integration methods. As can be seen, the spectral convergence in the angular direction of the proposed mixed method is very close to that of the Fourier–Chebyshev method, and has much better convergence properties than the finite-volume method.

The corresponding test for the radial direction indicates, as expected, that the rate of convergence in this direction follows that of finite volume.

Note that the global precision of the solution obtained with this method will depend also on the smoothness of the solution being approximated.

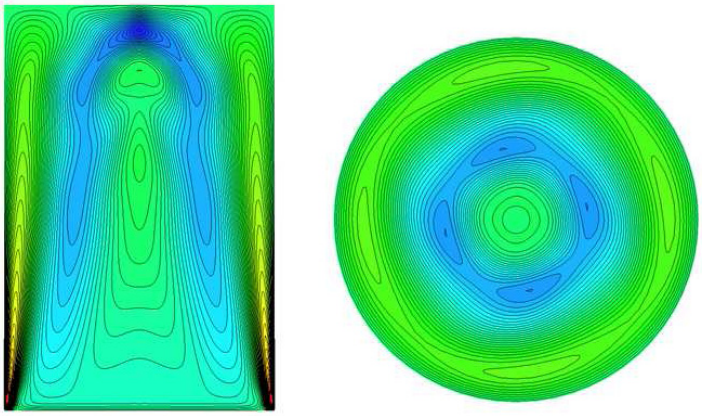

Figure 4. Instantaneous contours of the axial velocity of the $m = 4$ rotating wave at $Re = 2800$ and $\Lambda = 3.0$ in a meridional plane (left) and a horizontal plane at $z = 0.8\Lambda$ (right).

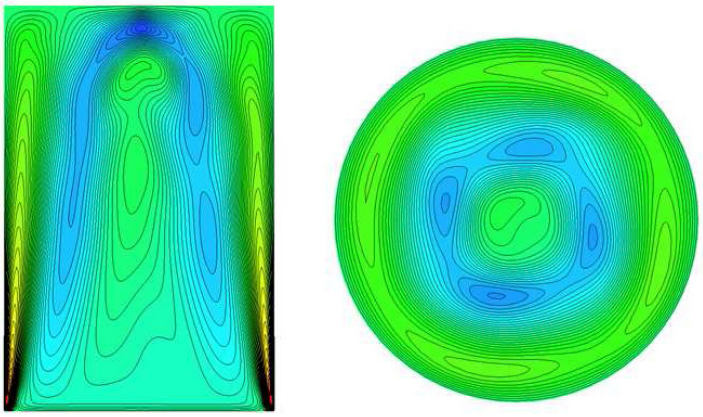

Figure 5. Instantaneous contours of the axial velocity of the modulated rotating wave with $m = 4$ and $m = 1$ at $Re = 3000$ and $\Lambda = 3.0$ in a meridional plane (left) and a horizontal plane at $z = 0.8\Lambda$ (right).

5.2. Vortex breakdown in a cylindrical tank with a rotating lid

The second example is the study of vortex breakdown in a cylinder driven by a rotating bottom. The flow is characterized by the aspect ratio $\Lambda = H/R$ where H is the height and R the radius, and the Reynolds number is defined by $Re = \Omega R^2/\nu$, where Ω is the angular velocity. Using a projection scheme for the velocity–pressure decoupling and a Legendre–Fourier approximation for the space variables, at $Re = 2730$ for $\Lambda = 3.0$ axisymmetric flow losses stability to an $m = 4$ rotating wave solution (Marques and Lopez 2001). On increasing Re to 2900, a second bifurcation to a modulated rotating wave takes place, introducing an $m = 1$ mode that manifests itself near the axis. The results obtained with the method proposed here are illustrated in figures 4 and 5. All major features described in previous studies are correctly captured by the present model. Figure 4 shows contours of the axial velocity in a meridional

plane and in a horizontal plane at $z = 0.8\Lambda$ for $Re = 2800$ and $\Lambda = 3.0$. The mode $m = 4$ flow is clearly observed and is confined to the region near the jet close to the lateral wall, as expected.

When the Reynolds number is increased, a second instability occurs and a modulated rotating wave that causes a precession with an $m = 1$ mode near the axis of symmetry appears. This flow at $Re = 3000$ is illustrated in figure 5 where the secondary instability is well developed. The flow close to the lateral wall displays an $m = 4$ distribution, while the flow near axis of the cylinder is clearly nonaxisymmetric. The agreement with the results of Marques and Lopez (2001) is very good.

6. Conclusions

A technique to solve the Navier–Stokes equations in cylindrical geometries with rigid boundary conditions that combines the advantages of the azimuthal periodicity and accuracy of the spectral methods with the possibility of considering discontinuous boundary conditions in the axial and/or radial directions has been proposed.

An important part of the method is a pressure-correction technique where the different Fourier components are required to satisfy mass conservation individually. In all tests, the method has been demonstrated to have the expected properties and is potentially useful for a variety of problems that might be more difficult to solve with other methods since Fourier methods preserve the symmetry of the continuous problems (O(2) or SO(2) depending on the boundary conditions) and so the proposed method might be useful in analyzing symmetry-breaking bifurcation problems.

Acknowledgments

JN acknowledges support through a doctoral scholarship from the Consejo Nacional de Ciencia y Tecnología (CONACYT), Mexico.

References

Barbosa E and Daube O 2005 *Comput. Fluids* **34** 950–71
Brown D L, Cortez R and Minion M L 2001 *J. Comput. Phys.* **168** 464–99
Canuto C, Hussaini M Y, Quarteroni A and Zhang T A 1988 *Spectral Methods in Fluid Dynamics* (Berlin: Springer)
Chorin A J 1968 *Math. Comput.* **22** 745–62
Eggels J G M, Unger F, Weiss M H, Westerweel J, Adrian R J, Friedrich R and Nieuwstadt F T M 1994 *J. Fluid Mech.* **268** 175–210
Fukagata K and Kasagi N 2002 *J. Comput. Phys.* **181** 478–98
Gottlieb D and Orzag S 1977 *Numerical Analysis of Spectral Methods: Theory and Applications* (Philadelphia, PA: SIAM)
Lopez J M, Marques F, Mercader I and Batiste O 2007 *J. Fluid Mech.* **590** 187–208
Marques F and Lopez J M 2001 *Phys. Fluids* **13** 1679–82
Mercader I, Batiste O and Alonso A 2010 *Comput. Fluids* **39** 215–24
Patankar S V and Spalding D B 1972 *Int. J. Heat Mass Transfer* **15** 1787–806
Peyret R 2002 *Spectral Methods for Incompressible Viscous Flow* (New York: Springer)
Tuckerman L S 1989 *J. Comput. Phys.* **80** 403–41
Versteeg H K and Malalasekera W 1995 *An Introduction to Computational Fluid Dynamics: The Finite Volume Method* (Englewood Cliffs, NJ: Prentice-Hall)
Verzicco R and Orlandi P 1996 *J. Comput. Phys.* **123** 402–14